# Holonomic quantum computation in the ultrastrong-coupling regime of circuit QED

Yimin Wang,[1,2] Jiang Zhang,[1] Chunfeng Wu,[3] J. Q. You,[1,*] and G. Romero[4]

[1]*Quantum Physics and Quantum Information Division, Beijing Computational Science Research Center, Beijing 100193, China*
[2]*College of Communications Engineering, PLA University of Science and Technology, Nanjing 210007, China*
[3]*Pillar of Engineering Product Development, Singapore University of Technology and Design, 8 Somapah Road, Singapore 487372*
[4]*Departamento de Física, Universidad de Santiago de Chile (USACH), Avenida Ecuador 3493, 9170124, Santiago, Chile*

We present an experimentally feasible scheme to implement holonomic quantum computation in the ultrastrong-coupling regime of light-matter interaction. The large anharmonicity and the $\mathbb{Z}_2$ symmetry of the quantum Rabi model allow us to build an effective three-level $\Lambda$-structured artificial atom for quantum computation. The proposed physical implementation includes two gradiometric flux qubits and two microwave resonators where single-qubit gates are realized by a two-tone driving on one physical qubit, and a two-qubit gate is achieved with a time-dependent coupling between the field quadratures of both resonators. Our work paves the way for scalable holonomic quantum computation in ultrastrongly coupled systems.

## I. INTRODUCTION

The extensive progress in quantum information science has motivated continuous demand for implementing high-fidelity quantum operations. Holonomic quantum computation (HQC) represents a promising approach to achieve this goal because of its intrinsic noise-resilience features [1,2]. The holonomic gates can be achieved by using either Abelian [3,4] or non-Abelian [5,6] geometric phases. The Abelian approach [7–9] utilizes quantum two-level systems (qubits) as elementary units, and the underlying idea is to choose a pair of orthogonal states that will evolve cyclically. In contrast, the non-Abelian approach [1,10] embeds qubits in a proper subspace of the total Hilbert space. Recently, a scheme to build fast holonomic gates through the non-Abelian approach has been proposed in Refs. [2,11]. The advent of this idea has triggered off a set of new proposals [12,13]. Apart from the theoretical interest, high fidelity gates based on fast HQC schemes have been demonstrated in different systems such as transmon-based superconducting qubits [14], NMR systems [15], and diamond NV centers [16,17].

On the other hand, the light-matter interaction has been the focus of interest in recent years owing to the experimental realizations of the ultrastrong-coupling (USC) regime [18–24]. In this case, the light-matter coupling strength is comparable to the cavity and the qubit frequencies [25], and in the dipolar approximation, it is described by the quantum Rabi model (QRM) [26,27]. Apart from the fundamental interest of the USC regime, it has been intensively studied for demonstrating novel quantum optics phenomena [28–32], implementing quantum information tasks [33,34], as well as fast quantum computation [35–39] within circuit quantum electrodynamics (QED) [40,41]. The latter provides a promising solid-state architecture for performing quantum computation due to the desirable properties of superconducting qubits, such as long coherence times, and most importantly, its controllability and scalability [42].

Meanwhile, many efforts have also been made to implement HQC in the cavity QED system with natural atoms [43] and artificial atoms [44], as well as the circuit QED system with superconducing qubits [45]. While the HQC scheme in Ref. [43] is performed adiabatically, the schemes in Refs. [44,45] are designed in a nonadiabatic fashion in addition to their decoherence-free subspace (DFS) encoding, and thus integrate both the noise resilience of DFS and the operational robustness of holonomies. However, all of those schemes [43–45] are based on the strong coupling of light-matter interaction, which can be well described by the Jaynes-Cummings model. To the best of knowledge, so far no scheme has ever been proposed to construct holonomic gates in the ultrastrong-coupling regime with the quantum Rabi model. Ultrastrong coupling offers the possibility for ultrafast quantum gate operations even in the time scale of subnanosecond [39], therefore, the realization of HQC in USC is of particular interest yet challenging.

In this work, we propose an experimentally feasible scheme to implement universal nonadiabatic HQC in the USC regime of light-matter interaction. The large anharmonicity and the $\mathbb{Z}_2$ symmetry of the QRM allow us to construct an effective three-level $\Lambda$-type system for quantum computing. We show that noncommuting single-qubit holonomic gates can be obtained by means of a two-tone driving on one physical qubit, and nontrivial two-qubit holonomic gates can be achieved with a time-dependent coupling between the field quadratures of two bosonic modes. Moreover, we discuss the physical implementation by considering two gradiometric flux qubits each galvanically coupled to its transmission line resonator, which are then connected to each other through a superconducting quantum interference device. Compared to the existing proposals for implementing HQC in circuit QED, the strategy we pursue is different in the sense that we exploit the discrete $\mathbb{Z}_2$ symmetry of the quantum Rabi model instead of the continuous U(1) symmetry of the Jaynes-Cummings model. Therefore, our proposal works well in the ultrastrong-coupling regime, and it may find compelling applications for quantum information processing in ultrastrong-coupling and deep strong-coupling regimes for various systems.
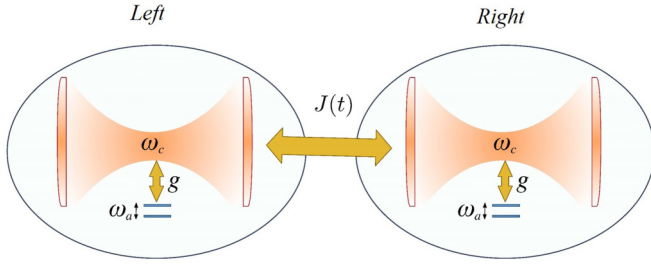
———————
*jqyou@csrc.ac.cn

FIG. 1. Schematic representation of our model. A system of a single qubit and a single cavity mode that interact in the ultrastrong-coupling regime constitutes the quantum Rabi system. The interaction between the two quantum Rabi systems is mediated by cavities through a time-dependent coupling of strength $J(t)$.

## II. SELECTION RULES IN THE QUANTUM RABI MODEL

The model that we consider is schematically depicted in Fig. 1. It includes two ultrastrongly coupled qubit-cavity systems, which interact via a time-dependent coupling of strength $J(t)$. Each ultrastrongly coupled system, onwards called quantum Rabi system (QRS), is described by

$$H_p = \hbar\omega_c a^\dagger a + \hbar\frac{\omega_a}{2}\sigma_z + \hbar g\sigma_x(a^\dagger + a), \quad (1)$$

where $\omega_a, \omega_c$, and $g$ stand for the qubit frequency, cavity frequency, and the qubit-resonator coupling strength, respectively. In addition, $a(a^\dagger)$ is the bosonic annihilation (creation) operator, and $\sigma_z$, $\sigma_x$ are the Pauli matrices of the qubit.

In the ultrastrong-coupling regime [46,47], which is characterized by the ratio range $0.1 \lesssim g/\omega_c < 1$, the bosonic field and the qubit merge into dressed-state systems that feature the discrete $\mathbb{Z}_2$ symmetry, as shown in Fig. 2, where we plot the energy spectrum of the quantum Rabi model as a function of the coupling strength $g/\omega_c$. This symmetry is characterized
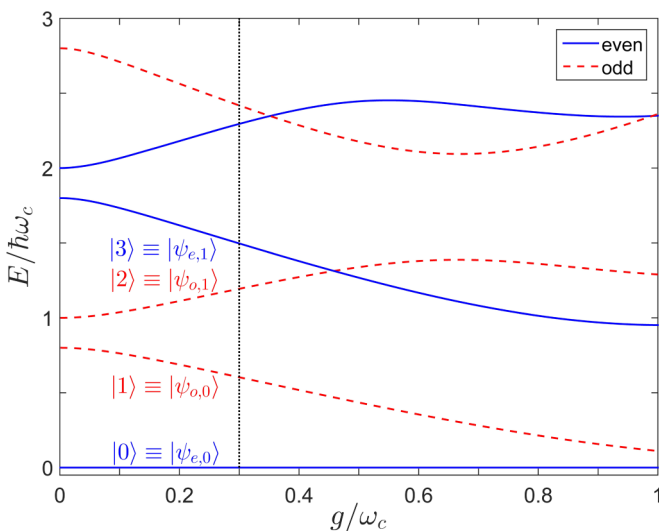


FIG. 2. Energy levels of the quantum Rabi model as a function of the dimensionless parameter $g/\omega_c$ with $\omega_a/\omega_c = 0.8$. Energies are rescaled in order to set the ground level to zero. The parity of the corresponding eigenstates is identified, continuous-blue line for even states and dashed-red lines for odd states.

by the parity operator $\mathcal{P} = e^{i\pi(a^\dagger a + \sigma_+\sigma_-)}$, such that $\mathcal{P}|\psi_e\rangle = |\psi_e\rangle$, $\mathcal{P}|\psi_o\rangle = -|\psi_o\rangle$. Note that in Fig. 2, even ($|\psi_e\rangle$) and odd ($|\psi_o\rangle$) eigenstates are represented by continuous-blue and dashed-red lines, respectively. The QRM can be rewritten as

$$H_p = \sum_{s=0} \hbar\omega_s|s\rangle\langle s|, \quad (2)$$

where we consider both even and odd parity states together and labeled them as eigenstates $|s\rangle$ of increasing energy $\hbar\omega_s$.

Formally, the parity in quantum mechanics is intimately related to the selection rules. For the QRM it can be shown that the matrix elements of an even operator are zero between states of different parity, $\langle\psi_e|\mathcal{A}_e|\psi_o\rangle = \langle\psi_o|\mathcal{A}_e|\psi_e\rangle = 0$, while the matrix elements of an odd operator are zero between states of equal parity $\langle\psi_e|\mathcal{A}_o|\psi_e\rangle = \langle\psi_o|\mathcal{A}_o|\psi_o\rangle = 0$. Also, from Fig. 2, we see that the spectrum is anharmonic enough such that the dressed states may be used as a computational basis for quantum information processing. In particular, when $g/\omega_c = 0.3$, one can build an effective three-level system by choosing the lowest three levels, $|0\rangle \equiv |\psi_{e,0}\rangle$, $|1\rangle \equiv |\psi_{o,0}\rangle$, and $|2\rangle \equiv |\psi_{o,1}\rangle$ to implement holonomic quantum computation schemes.

## III. SINGLE-QUBIT GATE

In this section we show how to construct an arbitrary single-qubit gate in the dressed-state basis of the quantum Rabi model with a nonadiabatic non-Abelian scheme [2]. We choose the two lower levels $|0\rangle$ and $|1\rangle$ to form the qubit subspace $\mathcal{S}_1(0) \equiv \{|0\rangle, |1\rangle\}$, leaving the upper level $|2\rangle$ as an auxiliary state.

In this encoding, the states $|0\rangle$ and $|2\rangle$ belong to different parity subspaces, such that the transitions between them can be induced by an odd parity operator, i.e., $\sigma_x$. Similarly, the states $|1\rangle$ and $|2\rangle$ have the same parity and the transition between them can be induced by an even parity operator such as $\sigma_z$. Therefore, a single-qubit holonomic quantum gate can be realized by making use of a two-tone driving scheme on the physical qubit. This can be modeled by the Hamiltonian,

$$H_d = \Omega_1(t)\cos(\bar{\omega}_1 t + \varphi_1)\sigma_x + \Omega_2(t)\cos(\bar{\omega}_2 t + \varphi_2)\sigma_z. \quad (3)$$

The qubit driving Hamiltonian Eq. (3) can be written in the dressed-state basis by using the completeness relation $I = \sum_s |s\rangle\langle s|$,

$$H_d = \Omega_1(t)\cos(\bar{\omega}_1 t + \varphi_1)\sum_{s,t} x_{st}|s\rangle\langle t|$$
$$+ \Omega_2(t)\cos(\bar{\omega}_2 t + \varphi_2)\sum_{s,t} z_{st}|s\rangle\langle t|, \quad (4)$$

where the transition elements are given by $x_{st} = \langle s|\sigma_x|t\rangle$ and $z_{st} = \langle s|\sigma_z|t\rangle$. Notice that according to the selection rule for even and odd operators, $x_{st} = 0$ if $|s\rangle$ and $|t\rangle$ belong to the same parity subspace, and $z_{st} = 0$ if $|s\rangle$ and $|t\rangle$ belong to a different parity subspace. Furthermore, we can interpret the projector $|s\rangle\langle t|$ as a flip operator between dressed states of either equal or different parity depending on the nature of the system operator (in our case, either $\sigma_x$ or $\sigma_z$). Therefore, such a Hamiltonian Eq. (4) induces coherent excitation transfer between all the possible dressed states.
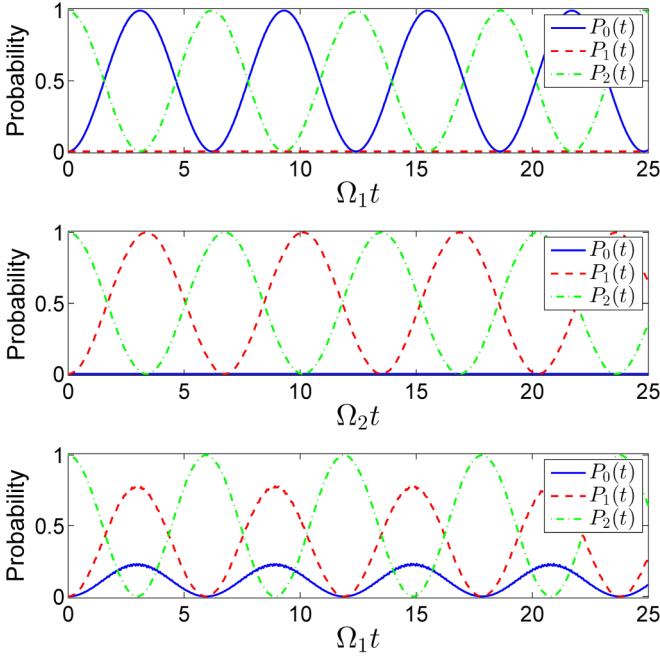
FIG. 3. Rabi oscillations for the lowest three dressed states in the quantum Rabi model by driving the physical qubit: (a) only in the **x** direction with strength $\Omega_1 = 0.02\omega_{20}$, $\Omega_2 = 0$; (b) only in the **z** direction with strength $\Omega_1 = 0$, $\Omega_2 = 0.02\omega_{21}$; (c) both in the **z** and **x** directions with strengths $\Omega_1 = \Omega_2 = 0.02\omega_{21}$. $P_i(t)$ ($i = 0,1,2$) is the probability of the state $|i\rangle$ as a function of time. The parameters are $\omega_a = 0.8\omega_c$, $g = 0.3\omega_c$, and driving frequencies $\bar{\omega}_1 = \omega_{21}$, $\bar{\omega}_2 = \omega_{20}$.

As we have shown in Fig. 2, for $g/\omega_c \leqslant 1$, the energy spectrum of the quantum Rabi system has a large anharmonicity such that one can access one particular transition frequency $\omega_{ts} = \omega_t - \omega_s$. Let us consider the total Hamiltonian $H = H_p + H_d$, and we move to the interaction picture with respect to the Rabi Hamiltonian in Eq. (2). If the condition $|\Omega_j(t)| \ll \min\{|\omega_{t,s}|, \bar{\omega}_j\}$ is satisfied, one can apply the RWA and neglect fast oscillating terms. Moreover, when bringing the frequency of the driving close to resonance with the transitions in which we are interested, i.e., $\bar{\omega}_1 = \omega_{20}$ and $\bar{\omega}_2 = \omega_{21}$, the interaction Hamiltonian reads

$$H_I = \frac{\Omega_1(t)}{2} e^{-i\varphi_1} x_{20} |2\rangle\langle 0|$$
$$+ \frac{\Omega_2(t)}{2} e^{-i\varphi_2} z_{21} |2\rangle\langle 1| + \text{H.c.}, \quad (5)$$

with $x_{20} = \langle 2|\sigma_x|0\rangle$ and $z_{21} = \langle 2|\sigma_z|1\rangle$. Therefore, by engineering the driving amplitudes and frequencies, Rabi oscillations between two specific dressed states can be performed.

In Fig. 3, we show Rabi oscillations for the lowest three dressed states in the quantum Rabi model. This simulation has been performed by making use of the full Hamiltonian $H = H_p + H_d$. As shown in Fig. 3(a), by driving the qubit in the $\sigma_x$ direction on resonance with the transition $\bar{\omega}_1 = \omega_{20}$, we observe Rabi oscillations between the two different parity states $|2\rangle$ and $|0\rangle$. Similarly, by driving the qubit in the $\sigma_z$ direction on resonance with the transition $\bar{\omega}_2 = \omega_{21}$, the complete population transfer between the two same parity states $|2\rangle$ and $|1\rangle$ is shown in Fig. 3(b). Moreover, by tuning

the driving frequency and amplitude to make both $\sigma_x$ and $\sigma_z$ rotations, we may have full control of any structured three-level system built from the dressed states of the quantum Rabi model, as shown in Fig. 3(c). In this manner, we are able to implement the effective Hamiltonian in Eq. (5).

Now we show how to construct an arbitrary holonomic single-qubit gate with the effective Hamiltonian $H_I$. By setting $\Omega^2(t) = (\Omega_1^2(t)|x_{20}|^2 + \Omega_2^2(t)|z_{21}|^2)/4$, $\varphi = \varphi_2 - \varphi_1$, and $\theta = -2\arctan[(\Omega_1(t)x_{20})/(\Omega_2(t)z_{21})]$, we can rewrite Eq. (5) as follows:

$$H_I = \Omega(t)\left(e^{i\varphi}\sin\frac{\theta}{2}|2\rangle\langle 0| - \cos\frac{\theta}{2}|2\rangle\langle 1| + \text{H.c.}\right). \quad (6)$$

In this case, we construct a $\Lambda$-system Hamiltonian in the dressed-state basis, from which an arbitrary single-qubit holonomic gate can be obtained. The effective Hamiltonian $H_I$ in Eq. (6) can be recast as the auxiliary state $|2\rangle$ coupled to the bright state $|b\rangle = e^{-i\varphi}\sin\frac{\theta}{2}|0\rangle - \cos\frac{\theta}{2}|1\rangle$ and decoupled from the dark state $|d\rangle = e^{i\varphi}\sin\frac{\theta}{2}|1\rangle + \cos\frac{\theta}{2}|0\rangle$. Initially, quantum information is stored in the qubit states of subspace $\mathcal{S}_1(0)$. When $H_I$ is applied, the subspace $\mathcal{S}_1$ is driven out of $\mathcal{S}_1(0)$, and we obtain the Rabi oscillation between states $|b\rangle$ and $|2\rangle$ with Rabi frequency of $\Omega(t)$. When the condition $\int_0^\tau \Omega(t)\mathbf{d}t = \pi$ is satisfied, the system states return to the original subspace $\mathcal{S}_1(0)$ after a cyclic evolution. The corresponding unitary operator $U_I(\tau)$ acting on $\mathcal{S}_1(0)$ reads $U_I(\tau) = \mathbf{n} \cdot \sigma$, where $\mathbf{n} = (\sin\theta\cos\varphi, \sin\theta\sin\varphi, \cos\theta)$ and $\sigma = (\sigma_x, \sigma_y, \sigma_z)$ being Pauli operators [2]. It is clear that two noncommuting single-qubit holonomic quantum gates can be achieved based on $U_I(\tau)$. Moreover, there is no dynamical contribution to $U_I(\tau)$ since $\langle m|H_I|n\rangle = 0$ ($m,n \in \mathbb{N}$) and hence $\langle m(t)|H_I|n(t)\rangle = 0$. The result shows the pure geometric nature of the obtained gate. Therefore, the desired single-qubit gates for universal quantum computation can be implemented in our system based on the nonadiabatic non-Abelian scheme [2,11].

The holonomic single-qubit gate performance under loss mechanisms in the ultrastrongly coupled system can be studied by means of the time-convolutionless projection operator method [48]. In this approach the master equation reads

$$\dot{\rho} = \frac{1}{i\hbar}[H_s, \rho]$$
$$+ \sum_{n=z,x,c}(U_n\rho S_n + S_n\rho U_n^\dagger - S_n U_n\rho - \rho U_n^\dagger S_n), \quad (7)$$

where $S_n$ are Hermitian system operators, and the operators $U_n$ are defined as

$$U_n = \int_0^\infty d\tau\, \nu_n(\tau) e^{-(i/\hbar)H_s\tau} S_n e^{(i/\hbar)H_s\tau},$$

$$\nu_n(\tau) = \int_{-\infty}^\infty d\omega \frac{\gamma_n(\omega)}{2\pi}[\bar{N}_n(\omega)e^{i\omega\tau} + (\bar{N}_n(\omega) + 1)e^{-i\omega\tau}].$$
$$(8)$$

Here, we consider independent thermal baths for each loss mechanism acting on the system described by the Hamiltonian $H_s(t) = \Omega(t)(\Upsilon_0|2\rangle\langle 0| + \Upsilon_1|2\rangle\langle 1| + \text{H.c.})$ [cf. Eq. (6)]. In our simulation we include loss mechanisms acting on the dressed-state system via transversal noise ($\gamma_x$), longitudinal
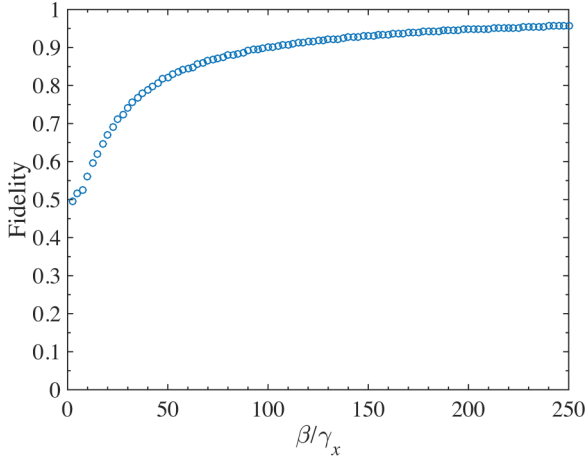
FIG. 4. Performance of the Hadamard gate under loss mechanisms acting upon the ultrastrongly coupled system. The fidelity is averaged on an ensemble of 4000 input states uniformly distributed over the Bloch sphere. In this simulation we have considered parameters $g = 0.3\omega_c$, $\omega_a = 0.8\omega_c$, $\gamma_x = \gamma_z = \gamma_c = 10^{-2}\omega_c$.

noise ($\gamma_z$), and noise acting on the field quadrature ($\gamma_c$), through operators $S_x = \sigma_x$, $S_z = \sigma_z$, and $S_c = a + a^\dagger$, respectively. In our treatment, each loss mechanism is described by independent thermal baths with bare loss rates $\gamma_j$. This leads to $\gamma_j(\omega) = (\gamma_j/\omega_j)\omega\Theta(\omega)$, where $\Theta(\omega)$ is the Heaviside step function.

Following Ref. [2] we have studied the performance of the Hadamard gate under loss mechanisms through the gate fidelity $F = \langle\chi|U^\dagger(C)\rho_{\text{out}}U(C)|\chi\rangle$, where $U(C) = (\sigma_x + \sigma_z)/\sqrt{2}$, and $\rho_{\text{out}}$ is the density matrix of the output state obtained from the master equation (7). The gate fidelity is computed numerically for 4000 input states $|\chi\rangle$, uniformly distributed over the Bloch sphere. In $H_s(t)$, we choose $\Omega(t)(\Upsilon_0,\Upsilon_1) = \beta\text{sech}(\beta t)(1,(\sqrt{2}-1))/\sqrt{2(2-\sqrt{2})}$, and the pulse is truncated where the amplitude is $\beta/1000$, which gives the pulse with a length $\tau = (2/\beta)\text{arcsech}(1/1000)$. The result is shown in Fig. 4 for parameters $g = 0.3\omega_c$, $\omega_a = 0.8\omega_c$, and $\gamma_x = \gamma_z = \gamma_c = 10^{-2}\omega_c$. Note that loss mechanisms in the dressed-state basis, including even and odd operators in the parity Hilbert space, will induce a complete decay to the fundamental state $|0\rangle$ at a scale time of $\sim 100/\omega_c$. Despite this, if the pulse is sufficiently short compared with the decay time, i.e., $\beta/\gamma_x \gg 1$, the fidelity of the nonadiabatic gate approaches to unity.

## IV. TWO-QUBIT GATE

In what follows, we will demonstrate a nontrivial two-qubit gate by using a nonadiabatic Abelian scheme [9] in a four-dimensional space spanned by the encoded logic qubit states $\mathcal{S}_2 \equiv \{|0_l0_r\rangle, |1_l0_r\rangle, |0_l1_r\rangle, |1_l1_r\rangle\}$. This can be proven by considering two ultrastrongly coupled systems that interact via a time-dependent coupling strength $J(t)$, as depicted in Fig. 1. The Hamiltonian describing the whole system is composed of the sum of two quantum Rabi models and a coupling between

the field quadratures [49,50],

$$H_{\text{tot}} = H_{p,l} + H_{p,r} + H_{\text{int}},$$
$$H_{\text{int}} = \hbar J(t)(a_l^\dagger + a_l)(a_r^\dagger + a_r), \quad (9)$$

with $H_{p,j}$ ($j = l,r$) being the Hamiltonian for the left and right quantum Rabi system.

By using the completeness relation, the system Hamiltonian Eq. (9) can be rewritten as

$$H_{\text{tot}} = \sum_{s=0}\left(\hbar\omega_{s,l}|s_l\rangle\langle s_l| + \hbar\omega_{s,r}|s_r\rangle\langle s_r|\right) + \hbar J(t)$$

$$\times\left[\sum_{s_l,t_l>s_l}\left(f_{s_lt_l}|s_l\rangle\langle t_l| + \text{H.c.}\right)\right.$$

$$\left.\otimes\sum_{u_r,v_r>u_r}\left(f_{u_rv_r}|u_r\rangle\langle v_r| + \text{H.c.}\right)\right], \quad (10)$$

where $f_{s_jt_j} = \langle s_j|(a_j + a_j^\dagger)|t_j\rangle$, $j = l,r$, is the transition matrix elements for the left ($l$) and right ($r$) system. Here, we have used the fact that the transition matrix elements are zero between states of the same parity, i.e., $f_{s_js_j} = 0$. Similar to the single-qubit case, the operator $|s_j\rangle\langle t_j|$ is the raising operator for the left or the right system. Let us consider the interaction picture with respect to Hamiltonian $H_{p,l} + H_{p,r}$. In this case, the interaction Hamiltonian reads

$$H_{\text{int}}^I = \hbar J(t)\left[\sum_{s_l,t_l>s_l}\left(f_{s_lt_l}|s_l\rangle\langle t_l|e^{-i\omega_{t_ls_l}t} + \text{H.c.}\right)\right.$$

$$\left.\times\sum_{u_r,v_r>u_r}\left(f_{u_rv_r}|u_r\rangle\langle v_r|e^{-i\omega_{v_ru_r}t} + \text{H.c.}\right)\right], \quad (11)$$

where $\omega_{t_js_j} = \omega_{t,j} - \omega_{s,j} > 0$. In particular, the cavity-cavity coupling parameter can be a time-dependent function $J(t) = J_0(t)\cos(\omega_d t + \varphi_d)$. In this case, if one chooses the resonance condition for two specific dressed states, i.e., $\omega_d = \omega_{v_ru_r} - \omega_{t_ls_l}$ and the cavity-cavity coupling strength satisfies the condition $|J_0(t)| \ll \omega_{t_ls_l} + \omega_{v_ru_r}$, we can apply the rotating-wave approximation and the interaction Hamiltonian effectively reduces to

$$H_{\text{int}} = \hbar\frac{J_0(t)}{2}f_{s_lt_l}f_{u_rv_r}^*e^{-i\varphi_d}|s_l\rangle\langle t_l| \otimes |v_r\rangle\langle u_r| + \text{H.c.}. \quad (12)$$

It is clear that such a Hamiltonian produces entanglement and induces coherent excitation transfer between specific dressed states $|s_l\rangle$ and $|t_l\rangle$ of the left and the right systems [50]. It is worth noting that the coupling operator $(a_l^\dagger + a_l)(a_r^\dagger + a_r)$ is an odd operator for the left and right quantum Rabi system individually, so it only induces transitions between states with opposite parity. Specifically, if we choose $\omega_d = \omega_{1_r0_r} - \omega_{1_l0_l}$, the system can be effectively described:

$$H_{\text{int}} = \hbar\frac{J_0(t)}{2}f_{0_l1_l}f_{0_r1_r}^*e^{-i\varphi_d}|0_l1_r\rangle\langle 1_l0_r| + \text{H.c.}, \quad (13)$$

which gives the interaction between two specific states $|0_l1_r\rangle$ and $|1_l0_r\rangle$. Meanwhile, Eq. (13) is our target Hamiltonian for the two-qubit HQC with the lowest three states in the dressed state basis. The interaction Hamiltonian (13) also indicates

that, out of the nine possible tensor states in the Hilbert space of the total system $\mathcal{H} = \mathcal{H}_{p,l} \otimes \mathcal{H}_{p,r}$, there are only two states that are correlated. This restricts us to a two-dimensional subspace which is spanned by vectors $\{|1_l 0_r\rangle, |0_l 1_r\rangle\}$, and allows us to demonstrate a two-qubit gate based on Abelian geometric phases. To illustrate our scheme, we encode the states $|1_l 0_r\rangle$ and $|0_l 1_r\rangle$ into logical single-qubit states $|1\rangle_L$ and $|0\rangle_L$, respectively. In the logical representation, Eq. (13) reads

$$H_{\text{int}} = \hbar \frac{J_0(t)}{2} f_{0_l 1_l} f_{0_r 1_r}^* (\cos \varphi_d \, S_x + \sin \varphi_d \, S_y), \quad (14)$$

where $S_x$ and $S_y$ are Pauli operators on the logical basis.

In what follows, we demonstrate a nontrivial two-qubit gate based on the Hamiltonian Eq. (14) according to the nonadiabatic Abelian scheme presented in Ref. [9]. A geometric phase shift gate $U_\beta$ acting on the eigenstates of $S_x$, namely $|\pm\rangle_L = (|0\rangle_L \pm |1\rangle_L)/\sqrt{2}$, can be achieved by letting the system evolve along a cyclic path based on properly designed four-step evolution up to a global phase. *Step 1*. By setting $\varphi_d = \pi/2$, we apply a rotation $e^{i\pi S_y/4}$ to the basis, changing the states from $|+\rangle_L$ and $|-\rangle_L$ to $|0\rangle_L$ and $-|1\rangle_L$, respectively. *Step 2*. By setting $\varphi_d = 0$, the states $|0\rangle_L$ and $|1\rangle_L$ are swapped with each other by a rotation $e^{i\pi S_x/2}$. *Step 3*. With a proper choice of the parameter $\varphi_d = \beta \neq m\pi$ ($m \in \mathbb{N}$), we evolve the states from $|0\rangle_L$ and $|1\rangle_L$ to $e^{i\beta}|1\rangle_L$ and $e^{-i\beta}|0\rangle_L$ respectively, by a rotation $e^{i\pi(\cos \beta S_x + \sin \beta S_y)/2}$. *Step 4*. By choosing $\varphi_d = \pi/2$ again, the resulting states $|0\rangle_L$ and $-|1\rangle_L$ can be changed back to $-|+\rangle_L$ and $|-\rangle_L$ by using the rotation $e^{-i\pi S_y/4}$, eliminating the minus sign obtained in the first step. Therefore, the system undergoes a cyclic evolution,

$$|+\rangle_L \rightarrow |0\rangle_L \rightarrow |1\rangle_L \rightarrow e^{-i\beta}|0\rangle_L \rightarrow e^{-i\beta}|+\rangle_L, \quad (15)$$

$$|-\rangle_L \rightarrow -|1\rangle_L \rightarrow -|0\rangle_L \rightarrow -e^{i\beta}|1\rangle_L \rightarrow e^{i\beta}|-\rangle_L, \quad (16)$$

and the obtained geometric phase shift gate $U_\beta$ written in the states $|\pm\rangle_L$ is of the following form,

$$U_\beta = \begin{pmatrix} e^{-i\beta} & 0 \\ 0 & e^{i\beta} \end{pmatrix}. \quad (17)$$

There is no dynamical phase accompanied during the cyclic evolution since the evolution is along geodesic lines. Equation (17) is nothing but a nontrivial two-qubit gate in the basis $\{|0_l 0_r\rangle, |1_l 0_r\rangle, |0_l 1_r\rangle, |1_l 1_r\rangle\}$ with

$$U_2 = \begin{pmatrix} 1 & 0 & 0 & 0 \\ 0 & \cos \beta & -i \sin \beta & 0 \\ 0 & -i \sin \beta & \cos \beta & 0 \\ 0 & 0 & 0 & 1 \end{pmatrix}. \quad (18)$$

It is apparent that $U_2$ is nontrivial when $\beta \neq m\pi$ with $m \in \mathbb{N}$. Together with the noncommuting single-qubit gates, we have demonstrated a universal set of holonomic quantum gates for the ultrastrongly coupled system.

## V. PHYSICAL IMPLEMENTATION

Here, we propose the use of a gradiometric flux qubit with a tunable gap galvanically connected to a cavity (see
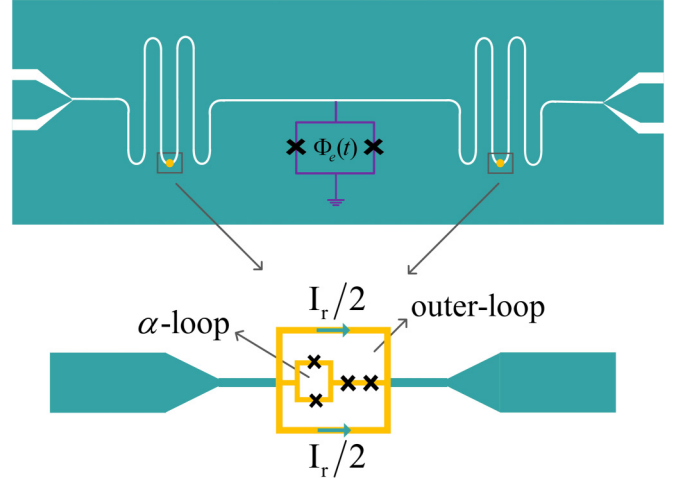


FIG. 5. Schematic of circuit QED design for the holonomic quantum computation. Two transmission line resonators (cavities) are grounded through a SQUID. Each cavity is galvanically coupled to a gradiometric tunable-gap flux qubit, that is constituted by four Josephson junctions. The time-dependent interaction between two resonators can be realized by modulating the external magnetic flux $\Phi_e(t)$ through the SQUID.

Fig. 5) to implement HQC. This circuit QED architecture in the strong-coupling regime has been implemented in [51]. Also, the ultrastrong-coupling regime may be achieved by implementing a longer and thinner shared line between the gradiometric flux qubit and the microwave resonator [52].

We stress that the gradiometric configuration is unaffected by homogenous magnetic fields, so it has the advantage to overcome flux crosstalk [51]. Also, an inhomogenous magnetic field in the outer loop of the flux qubit enables the coupling to a microwave resonator. The additional $\alpha$ loop in the gradiometric configuration allows for a tunable qubit gap. This mechanism is completely independent of the flux line that controls the frustration parameter in the outer loop [51,52]. Therefore, our two-tone driving scheme for the single-qubit gate may be implemented in the gradiometric qubit by applying two independent magnetic fluxes of different frequencies to the outer loop and the $\alpha$ loop [37].

The time-dependent coupling $J(t)$ between the two cavities can be implemented by means of a superconducting quantum interference device (SQUID) [49], threaded by an external flux $\Phi_e(t)$, as shown in Fig. 5. Although the effective cavity length is oscillating with small deviations from its average value, we can still consider the system as a single-mode resonator; see Ref. [49] for a detailed discussion. In particular, the specific form of cavity-cavity coupling strength $(J(t) = J_0(t) \cos(\omega_d t + \varphi_d))$ required for the two-qubit gate, may be achieved by choosing the time-dependent external magnetic flux $\Phi_e(t)$ to be composed of the sum of a small amplitude-modulated signal oscillating at the driving frequency $\omega_d$ and a constant offset $\bar{\Phi}$, namely, $\Phi_e(t) = \bar{\Phi} + \Delta\Phi \, \Omega(t) \cos(\omega_d t + \varphi_d)$. By controlling the driving frequency $\omega_d$, it will allow us to selectively activate the interaction between two specific energy states of the system and to obtain

the effective Hamiltonian Eq. (13) for the two-qubit gate; see the appendix for a detailed discussion.

## VI. CONCLUSION

In conclusion, we have presented a proposal to implement a holonomic quantum computation scheme in the ultrastrong-coupling regime of circuit QED. The effective three-level $\Lambda$ artificial atom to carry out the quantum gate operations is built from the eigenstates of the quantum Rabi model in the dressed-state basis, which is based on its large anharmonicity and the $\mathbb{Z}_2$ symmetry. Arbitrary non-Abelian single-qubit gates can be achieved by selectively driving the physical qubit in both $\sigma_x$ and $\sigma_z$ directions with different frequencies. A nontrivial Abelian two-qubit quantum phase gate can be demonstrated by controlling both the frequency and the amplitude of the time-dependent cavity-cavity coupling strength $J(t) = J_0(t)\cos(\omega_d t + \varphi_d)$ between the field quadratures, and by performing a four-step cyclic evolution scheme. Furthermore, we have proposed an experimentally feasible circuit QED architecture for the physical implementation of our scheme. Here, each gradiometric tunable-gap flux qubit is connected galvanically to the center conductor of a transmission line resonator to reach the USC regime. The resonators are connected to the same edge of a grounded SQUID, which is surrounded by a time-dependent external magnetic flux. Our proposal provides novel applications of the ultrastrong-coupling regime of light matter for scalable holonomic quantum computation.

## APPENDIX

### 1. Quantization of the circuit model and its quantum dynamics

A detailed analysis of circuit quantization of Fig. 5 can be found in Ref. [49]. The full system Hamiltonian that includes the two quantum Rabi models and the resonator-resonator coupling reads

$$
\begin{aligned}
H = {} & H_{p,l} + H_{p,r} + \hbar \sum_{j=l,r} \left[ \bar{J}_j + J_j(t)\cos(\omega_d t + \varphi_d) \right] \\
& \times (a_j + a_j^\dagger)^2 + \hbar \left[ \bar{J}_0 + J_0(t)\cos(\omega_d t + \varphi_d) \right] \\
& \times (a_l + a_l^\dagger)(a_r + a_r^\dagger),
\end{aligned} \tag{A1}
$$

with

$$
\bar{J}_j = \frac{\phi_0}{4I_c \cos\bar{\phi}} \frac{\omega_j}{Z_j^2 C_j}, \quad \bar{J}_0 = 2\sqrt{\bar{J}_l \bar{J}_r},
$$

$$
J_j(t) = \frac{\phi_0}{4I_c} \frac{\sin\bar{\phi}}{\cos^2\bar{\phi}} \frac{\omega_j}{Z_j^2 C_j} \Delta\phi\,\Omega(t), \quad J_0(t) = 2\sqrt{J_l(t)J_r(t)}.
\tag{A2}
$$

The above circuit Hamiltonian is obtained by considering a weak harmonic magnetic flux with frequency $\omega_d$ applied to the SQUID, that is,

$$
\Phi_e(t) = \bar{\Phi} + \Delta\Phi\,\Omega(t)\cos(\omega_d t + \varphi_d), \tag{A3}
$$

with $\Delta\Phi \ll \bar{\Phi}$ and $\Omega(t)$ being the normalized temporal envelope of the applied flux. It implies $\bar{\phi} = \pi\bar{\Phi}/\Phi_0$ and $\Delta\phi = \pi\Delta\Phi/\Phi_0$.

Notice that the above Hamiltonian Eq. (A1) is different from the Hamiltonian discussed in the main text (9). In particular, except the time-depentent resonator-resonator coupling terms, the Hamiltonian (A1) also includes single-mode squeezing terms and time-independent coupling terms. Nonetheless, one can demonstrate that Eq. (A1) reduces to Eq. (11) if we consider realistic system parameters. In order to see this correspondence, let us assume identical resonators, $\omega_l = \omega_r = \omega_c$, with impedances $Z_j = 80\Omega$ and capacitances $C_j = 200$ fF. For the critical current of the SQUID we consider $I_c = 180\mu$A. Notice that recent experiments in circuit QED have considered critical currents in the range of $1 - 2\mu$A [53], however, one can increase the critical current to a larger value or even a few orders of magnitude into the $m$A regime by making the junctions bigger; this would involve a trilayer fabrication process [54,55]. Moreover, we consider a flat ($\Omega(t) = 1$) magnetic flux pulse applied to the SQUID with parameters $\bar{\phi} = \pi/4$ and $\Delta\phi = 0.1\bar{\phi}$. The reduced flux quantum is $\phi_0 = \hbar/(2e) = 3.2911 \times 10^{-16}$Wb.
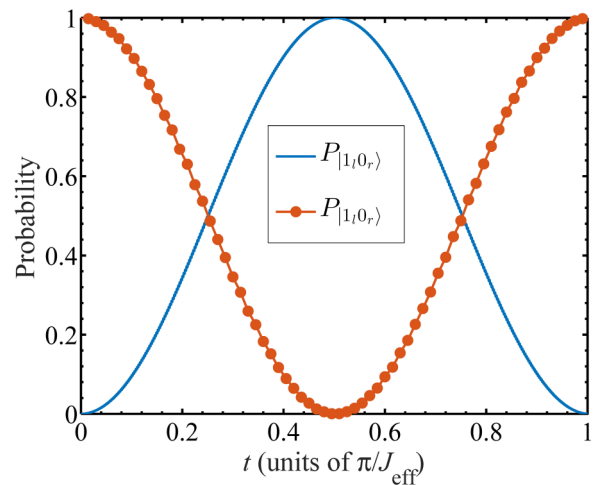


FIG. 6. Population inversion between states $|1_l 0_r\rangle$ and $|0_l 1_r\rangle$ for nonidentical quantum Rabi systems with parameters $\omega_l = 1$, $\omega_{a,l} = 0.8\omega_l$, $g_l = 0.3\omega_l$ for the left quantum Rabi system, and $\omega_r = 1$, $\omega_{a,r} = \omega_r$, $g_r = 0.9\omega_r$ for the right quantum Rabi system. These values lead to an effective cavity-cavity coupling strength $J_{\text{eff}} \approx 5.5 \times 10^{-4}\omega_r$. This simulation has been performed with the full Hamiltonian (A1) through the Runge-Kutta algorithm.

These parameters lead to $\bar{J}_j \approx 5 \times 10^{-4}\omega_c$, $\bar{J}_0 \approx 10^{-3}\omega_c$, $J_j \approx 4 \times 10^{-5}\omega_c$, and $J_0 \approx 8 \times 10^{-5}\omega_c$.

Now we consider the completeness relation for both quantum Rabi systems so that (A1) can be expressed as

$$H = \sum_{s=0} \left(\hbar\omega_{s,l}|s_l\rangle\langle s_l| + \hbar\omega_{s,r}|s_r\rangle\langle s_r|\right) + \sum_{j=l,r}\left[\bar{J}_j + J_j(t)\cos(\omega_d t + \varphi_d)\right]$$
$$\times \left\{\sum_{s_j,t_j>s_j}\left(X_{s_j t_j}|s_j\rangle\langle t_j| + X^*_{s_j t_j}|t_j\rangle\langle s_j|\right) + \sum_{s_j}X_{s_j s_j}|s_j\rangle\langle s_j|\right\}$$
$$+ \left[\bar{J}_0 + J_0(t)\cos(\omega_d t + \varphi_d)\right]\left\{\sum_{s_l,t_l>s_l}\left(f_{s_l t_l}|s_l\rangle\langle t_l| + \text{H.c.}\right) \otimes \sum_{u_r,v_r>u_r}\left(f^r_{u_r v_r}|u_r\rangle\langle v_r| + \text{H.c.}\right)\right\}, \tag{A4}$$

where $X_{s_j t_j} = \langle s_j|(a_j + a_j^\dagger)^2|t_j\rangle$ and $f_{s_j t_j} = \langle s_j|(a_j + a_j^\dagger)|t_j\rangle$. Notice that the single mode squeezing operator $(a_j + a_j^\dagger)^2$ is an even operator according to the parity symmetry of the system. It means that will connect states within the same parity subspace. Now, if we go to an interaction picture with respect to $H_{p,l} + H_{p,r}$, the Hamiltonian (A4) reads

$$H_I(t) = \sum_{j=l,r}\left[\bar{J}_j + J_j(t)\cos(\omega_d t + \varphi_d)\right]\left\{\sum_{s_j,t_j>s_j}\left(e^{-i\omega_{t_j s_j}t}X_{s_j t_j}|s_j\rangle\langle t_j| + e^{i\omega_{t_j s_j}t}X^*_{s_j t_j}|t_j\rangle\langle s_j|\right) + \sum_{s_j}X_{s_j s_j}|s_j\rangle\langle s_j|\right\}$$
$$+ \left[\bar{J}_0 + J_0(t)\cos(\omega_d t + \varphi_d)\right]\left\{\sum_{s_l,t_l>s_l}\left(e^{-i\omega_{t_l s_l}t}f_{s_l t_l}|s_l\rangle\langle t_l| + \text{H.c.}\right) \otimes \sum_{u_r,v_r>u_r}\left(e^{-i\omega_{t_r s_r}t}f_{u_r v_r}|u_r\rangle\langle v_r| + \text{H.c.}\right)\right\}. \tag{A5}$$

If we restrict the three lowest energy levels for each quantum Rabi system, the above Hamiltonian reads

$$H_I(t) = \sum_{j=l,r}\left[\bar{J}_j + J_j\cos(\omega_d t + \varphi_d)\right]\left\{\left(e^{-i\omega_{2_j 1_j}t}X_{1_j 2_j}|1_j\rangle\langle 2_j| + e^{i\omega_{2_j 1_j}t}X^*_{1_j 2_j}|2_j\rangle\langle 1_j|\right) + \sum_{s_j=0}^{2}X_{s_j s_j}|s_j\rangle\langle s_j|\right\}$$
$$+ [\bar{J}_0 + J_0\cos(\omega_d t + \varphi_d)]\left(e^{-i\omega_{1_l 0_l}t}f_{0_l 1_l}|0_l\rangle\langle 1_l| + e^{-i\omega_{2_l 0_l}t}f_{0_l 2_l}|0_l\rangle\langle 2_l| + \text{H.c.}\right)$$
$$\otimes \left(e^{-i\omega_{1_r 0_r}t}f_{0_r 1_r}|0_r\rangle\langle 1_r| + e^{-i\omega_{2_r 0_r}t}f_{0_r 2_r}|0_r\rangle\langle 2_r| + \text{H.c.}\right). \tag{A6}$$

For nonidentical quantum Rabi systems, the above Hamiltonian can produce single excitation transfer if the resonance condition for the driving frequency is $\omega_d = \omega_{1_r 0_r} + \bar{J}_r(X_{1_r 1_r} - X_{0_r 0_r}) - [\omega_{1_l 0_l} + \bar{J}_l(X_{1_l 1_l} - X_{0_l 0_l})]$. Notice that single-mode squeezing terms $\bar{J}_j X_{s_j s_j}$ produce energy shifts for each dressed state. Furthermore, the rotating-wave approximation holds under conditions $\bar{J}_j|X_{1_j 2_j}| \ll \omega_{2_j 1_j}$, $J_j|X_{1_j 2_j}| \ll |\omega_{2_j 1_j} \pm \omega_d|$, $J_j|X_{s_j s_j}| \ll \omega_d$, and $\bar{J}_0 f^*_{0_l 1_l}f_{0_r 1_r} \ll |\omega_{1_l 0_l} - \omega_{1_r 0_r}|$. The effective coupling strength between the two specific dressed states of the two quantum Rabi models is given by $J_{\text{eff}} = (J_0/2)f^*_{0_l 1_l}f_{0_r 1_r}$.

We have performed *ab initio* numerics by considering the Hamiltonian (A1). Figure 6 shows the population inversion between states $|1_l 0_r\rangle$ and $|0_l 1_r\rangle$ for nonidentical quantum Rabi systems; see the caption to check parameters. For simplicity we have taken $\varphi_d = 0$; its correspondence to Hamiltonian (13) discussed in the main text is quite clear.

[1] P. Zanardi and M. Rasetti, Phys. Lett. A **264**, 94 (1999).

[2] E. Sjöqvist, D. M. Tong, L. M. Andersson, B. Hessmo, M. Johansson, and K. Singh, New J. Phys. **14**, 103035 (2012).

[3] M. V. Berry, Proc. R. Soc. A **392**, 45 (1984).

[4] Y. Aharonov and J. Anandan, Phys. Rev. Lett. **58**, 1593 (1987).

[5] F. Wilczek and A. Zee, Phys. Rev. Lett. **52**, 2111 (1984).

[6] J. Anandan, Phys. Lett. A **133**, 171 (1988).

[7] J. A. Jones, V. Vedral, A. Ekert, and G. Castagnoli, Nature (London) **403**, 869 (2000).

[8] W. Xiang-Bin and M. Keiji, Phys. Rev. Lett. **87**, 097901 (2001).

[9] S.-L. Zhu and Z. D. Wang, Phys. Rev. Lett. **89**, 097902 (2002).

[10] L.-M. Duan, J. I. Cirac, and P. Zoller, Science **292**, 1695 (2001).

[11] G. F. Xu, J. Zhang, D. M. Tong, E. Sjöqvist, and L. C. Kwek, Phys. Rev. Lett. **109**, 170501 (2012).

[12] J. Zhang, T. H. Kyaw, D. M. Tong, E. Sjöqvist, and L. C. Kwek, Sci. Rep. **5**, 18414 (2015).

[13] J. Zhang, L. C. Kwek, E. Sjöqvist, D. M. Tong, and P. Zanardi, Phys. Rev. A **89**, 042302 (2014).

[14] A. A. Abdumalikov Jr., J. M. Fink, K. Juliusson, M. Pechal, S. Berger, A. Wallraff, and S. Filipp, Nature (London) **496**, 482 (2013).

[15] G. Feng, G. Xu, and G. Long, Phys. Rev. Lett. **110**, 190501 (2013).

[16] S. Arroyo-Camejo, A. Lazariev, S. W. Hell, and G. Balasubramanian, Nature Comm. **5**, 4870 (2014).

[17] C. Zu, W.-B. Wang, L. He, W.-G. Zhang, C.-Y. Dai, F. Wang, and L.-M. Duan, Nature (London) **514**, 72 (2014).

[18] A. A. Anappara, S. De Liberato, A. Tredicucci, C. Ciuti, G. Biasiol, L. Sorba, and F. Beltram, Phys. Rev. B **79**, 201303 (2009).

[19] G. Günter *et al.*, Nature (London) **458**, 178 (2009).

[20] Y. Todorov, A. M. Andrews, R. Colombelli, S. De Liberato, C. Ciuti, P. Klang, G. Strasser, and C. Sirtori, Phys. Rev. Lett. **105**, 196402 (2010).

[21] G. Scalari *et al.*, Science **335**, 1323 (2012).

[22] P. Forn-Díaz, J. Lisenfeld, D. Marcos, J. J. García-Ripoll, E. Solano, C. J. P. M. Harmans, and J. E. Mooij, Phys. Rev. Lett. **105**, 237001 (2010).

[23] T. Niemczyk *et al.*, Nature Phys. **6**, 772 (2010).

[24] Z. Chen *et al.*, arXiv:1602.01584.

[25] J. Casanova, G. Romero, I. Lizuain, J. J. García-Ripoll, and E. Solano, Phys. Rev. Lett. **105**, 263603 (2010).

[26] I. I. Rabi, Phys. Rev. **49**, 324 (1936).

[27] D. Braak, Phys. Rev. Lett. **107**, 100401 (2011).

[28] S. Ashhab and F. Nori, Phys. Rev. A **81**, 042311 (2010).

[29] A. Ridolfo, M. Leib, S. Savasta, and M. J. Hartmann, Phys. Rev. Lett. **109**, 193602 (2012).

[30] E. Sanchez-Burillo, D. Zueco, J. J. García-Ripoll,, and L. Martin-Moreno, Phys. Rev. Lett. **113**, 263604 (2014).

[31] L. Garziano, R. Stassi, V. Macrì, A. F. Kockum, S. Savasta, and F. Nori, Phys. Rev. A **92**, 063830 (2015).

[32] M. J. Hwang, R. Puebla, and M. B. Plenio, Phys. Rev. Lett. **115**, 180404 (2015).

[33] T. H. Kyaw, S. Felicetti, G. Romero, E. Solano, and L. C. Kwek, Sci. Rep. **5**, 8621 (2015).

[34] S. Felicetti, T. Douce, G. Romero, P. Milman, and E. Solano, Sci. Rep. **5**, 11818 (2015).

[35] P. Nataf and C. Ciuti, Phys. Rev. Lett. **107**, 190402 (2011).

[36] Y. D. Wang, P. Zhang, D. L. Zhou, and C. P. Sun, Phys. Rev. B **70**, 224515 (2004).

[37] Y. D. Wang, A. Kemp, and K. Semba, Phys. Rev. B **79**, 024502 (2009).

[38] Y. M. Wang, D. Ballester, G. Romero, V. Scarani, and E. Solano, Phys. Scr. T **147**, 014031 (2012).

[39] G. Romero, D. Ballester, Y. M. Wang, V. Scarani, and E. Solano, Phys. Rev. Lett. **108**, 120501 (2012).

[40] A. Wallraff, D. I. Schuster, A. Blais, L. Frunzio, R.-S. Huang, J. Majer, S. Kumar, S. M. Girvin, and R. J. Schoelkopf, Nature (London) **431**, 162 (2004).

[41] I. Chiorescu, P. Bertet, K. Semba, Y. Nakamura, C. J. P. M. Harmans, and J. E. Mooij, Nature (London) **431**, 159 (2004).

[42] R. Barends *et al.*, Nature (London) **508**, 500 (2014).

[43] A. Recati, T. Calarco, P. Zanardi, J. I. Cirac, and P. Zoller, Phys. Rev. A **66**, 032309 (2002).

[44] J. Zhou, W.-C. Yu, Y.-M. Gao, and Z. Y. Xue, Opt. Express **23**, 14027 (2015).

[45] Z. Y. Xue, J. Zhou, and Y. Hu, arXiv:1601.07219.

[46] C. Ciuti, G. Bastard, and I. Carusotto, Phys. Rev. B **72**, 115303 (2005).

[47] J. Bourassa, J. M. Gambetta, A. A. Abdumalikov, O. Astafiev, Y. Nakamura, and A. Blais, Phys. Rev. A **80**, 032109 (2009).

[48] H. P. Breuer and F. Petruccione, *The Theory of Open Quantum Systems* (Oxford University Press, Oxford, 2002).

[49] S. Felicetti, M. Sanz, L. Lamata, G. Romero, G. Johansson, P. Delsing, and E. Solano, Phys. Rev. Lett. **113**, 093602 (2014).

[50] D. Z. Rossatto, S. Felicetti, H. Eneriz, E. Rico, M. Sanz, and E. Solano, Phys. Rev. B **93**, 094514 (2016).

[51] M. J. Schwarz, J. Goetz, Z. Jiang, T. Niemczyk, F. Deppe, A. Marx, and R. Gross, New J. Phys. **15**, 045001 (2013).

[52] M. J. Schwarz, Ph.D thesis, Walther-Meisser Institut, Munich, 2015.

[53] C. M. Wilson, G. Johansson, A. Pourkabirian, M. Simoen, J. R. Johansson, T. Duty, F. Nori, and P. Delsing, Nature (London) **479**, 376 (2011).

[54] C. Wilson at Institute for Quantum Computing, University of Waterloo (private communication).

[55] L. Li, L. Frunzio, C. Wilson, and D. E. Prober, J. Appl. Phys. **90**, 3645 (2001).